Wireless Communication Through Microtubule Analogue Device: Noise-Driven Machines in the Bio-Systems

Komal Saxena, K. V. Karthik, Suryakant Kumar, D. Fujita and Anirban Bandyopadhyay

Abstract Looking beyond ionic communication in bio-systems that is limited to a narrow band of kHz frequency domain is our objective. Microtubule, a vital subcellular biomolecule found in almost all eukaryotic living systems, plays an important role in processing the cellular information. Therefore, here we introduce a microtubule analogue device, which wirelessly communicates with the neighboring microtubules and harvest energy from the noise present in the environment. The device is composed of spatially arranged lattice geometry with two different lattice parameters made of capacitors as tubulin protein analogue arranged on cylindrical shape structures. To demonstrate that the noise is harvested, both the devices are operated by noise, no ordered signal is applied in any measurement. Separation between both the devices is varied, while nearing the distance, the transmitted signal increases continuously and when they are taken further apart, the signal decreases gradually to null at ~140 cm. We image live, the generation and transmission of magnetic flux condensate between these two devices. This experiment is also repeated by inserting a magnetic shield 99.99% pure Ni sheet between two structures, which allows very less wireless transmission due to the shielding. The wireless communication frequency is in the range kHz–MHz.

Keywords Wireless power transfer · Magnetic condensate · Heat pipe effect Noise harvesting · Microtubule

K. Saxena · K. V. Karthik · S. Kumar · D. Fujita · A. Bandyopadhyay (✉)
Advanced Key Technologies Division, National Institute for Materials Science, 1-2-1 Sengen, Tsukuba, Ibaraki 3050047, Japan
e-mail: anirban.bandyo@gmail.com

K. Saxena
Microwave Physics Laboratory, Dayalbagh Educational Institute, Dayalbagh, Agra 282005, Uttar Pradesh, India

K. Ray et al. (eds.), *Engineering Vibration, Communication and Information Processing*, Lecture Notes in Electrical Engineering 478,
https://doi.org/10.1007/978-981-13-1642-5_64

1 Introduction

Wireless communication is projected to bring the next industrial revolution [1]. There are plenty of challenges and opportunities [2]. Specially, in the field of biomedical engineering, wireless nanobots can do wonderful surgery [3] and [4]. Even it is demonstrated that organic nanobots could be used to destroy cancer cells and destroy beta plaques of Alzheimer's patient [5].

Biological systems are known to transfer signals by diffusing ions and process information using chemical reactions—a major part of its interaction is played by the protein's mechanical transformation of secondary structures. Biomaterials are made up of various components each with different dielectric constants, protein resonance was first measured around 1930s [6, 7]. Therefore, they are not like a tuning fork vibrating at a single frequency; shift in resonance frequencies reveal much more than static response [8]. One could confine water molecules via hydration [9] for the resonance measurement. Resonance peaks is a set of frequency that could act as a marker for a protein [10]. Consequently during resonance measurement a protein responds in a nanocavity in a complex manner [11, 12]. Measurements were made even in superconducting cavity [13]. Dispersion relation of a material is its dielectric response as a function of frequency; it reveals how different kinds of dielectric constituents in a material dominate in absorbing energy and resonantly vibrating at different frequencies [14]. Resonance of proteins survives in living cells [15]. After 26 years, we performed a similar experiment with advanced tools on tubulin and microtubule inside a live neuron cell [16]. Cells are not just chemical fluids [17, 18]. Dielectric and electronic properties have one-to-one correspondence [19]. Ionic interactions mostly occur in the kHz frequency domain as ionic waves take a long time to clock. Since existing biology mostly focuses on the ionic and molecular interactions, it looks only into the milliseconds domain. If there are other events happening at different time domains, then molecular biology does not take into account those factors. In fact, giant protein structures responsible for ionic transfers are all made of dipoles, which vibrate at several hundreds of nanoseconds to microsecond periods. The Fourier transform of such signal shows resonance frequency peaks in the MHz frequency domain [20, 21]. However, these dipoles are made of functional groups, which vibrate in picoseconds to nanoseconds time domain; we see resonance peaks in the Fourier transform plot. We speculated that a biological phenomenon would not be limited to a narrow kHz frequency domain or milliseconds time domain. We proposed that biological systems would operate in different time domains simultaneously and those time domains are geometrically connected. In this context, we offered a resonance chain where triplet of triplet grouping of resonance frequencies would be the most predominant topology, integrating the vibrations of a biological system [22]. If that were true, multiple communication modes would operate simultaneously in a single biological system. Apart from ionic diffusion and electrical pulse passing through a solid medium, there is a possibility of wireless transmission of signals.

Wireless transmission could happen in two ways. First, an antenna and receiver system radiates and absorbs electromagnetic energy in its structure. Then, the materials involved could be dielectric resonators and/or cavity resonators. Second, transferring the magnetic fields over a short distance directly, this route is popularly depicted as Tesla coil [23]. In this route, there are two ways. First, two conducting coils are kept side by side, and current passes through them, then due to inductive coupling, the magnetic energy could transfer. Alternately, there could be a pair of parallel plates; due to capacitive coupling, they could transfer magnetic fields. Both capacitive and inductive routes are studied in detail. Both the routes require a current flow. However, we have seen that if ionic motions are restricted, biomaterials do not allow flow of current. In presence of fluids, it is impossible to study conductivity of biomaterials because ionic currents through water find a direct less resistive transmission route via water, so they reject the more difficult biomaterial route. Therefore, the observed high current (above microampere) originates from water conductivity and not from biomaterials. When we developed the trick to study biomaterials under limited water layer 3–5 nm, we found that the conductivity of a material decreases several orders of magnitude (300 GΩ–10^{15} Ω). Therefore, biological systems are nonconducting intrinsically. This finding argues that they are not fit for wireless communication in the conventional routes as they cannot allow flow of current. Neither, biomaterials could be classical antenna or receiver, nor they could be Tesla coils. Moreover, water damps the electromagnetic signals, so an electromagnetic signal cannot pass through. If there exists at all any possibility of wireless communication, the only option would be magnetic wireless transmission. However, we need to identify how a critical insulator could communicate wirelessly when it cannot allow flow of current through itself.

Recently, attempts are being made to find options of wireless communication beyond strong coupling, exploring ideas to avoid exponential decay of wireless transmission as a function of distance [24], coupling magnetic resonance [25], switching multiple coils to enhance efficiency [26], and range modulation [27]. Here, we are exploring a new idea, if ultralow power driven by noise could transmit magnetic energy between two nonconducting materials. Biomaterials are rich in spiral structures, starting from DNA, alfa-helices, microtubule, actin-like microfilaments and neurofilaments, and even collagen. They look like Tesla coils, the only problem is that they do not allow the flow of currents as we expect. Current flow through the biomaterials is of the order of a few picoamperes even if 1 V is applied across the device. It is nearly impossible to investigate a biomaterial from all directions; they have a few nm-wide sizes, and hence accessing different parts simultaneously is nearly impossible. For that reason, we make 10^6 times larger replica of microtubule, predicted to process information in 1982 [28] and verified in 2013 [29], keeping its structural parameters identical to its biological counterparts. Then, we carry out rigorous investigations to find out if there is at all any possibility that wireless electromagnetic or magnetic communication could happen. One problem is that a microtubule is made of several tubulin proteins arranged all along the surface of an ordered water crystal core [21]. Therefore, we need to find an analogue of protein constituents for its artificial replica. We do it simply by taking capacitors. Even we keep the value of

the capacitor 106 times (microtesla) the capacitance of a tubulin protein, which is ~0.1 pT. In Sect. 2, the formulation for analyzing the different parameters is given. In Sect. 3, the experimental setup to demonstrate the noise is harvested through a microtubule analogue device and the design is discussed. In Sect. 4, various results based on the harvesting noise and generations of magnetic flux are discussed.

2 Formulation and Design Concept

2.1 The Concept of Microtubule Analogue

Preparation of an analogue microtubule has been patented (an inductor made of arrayed capacitors [30]). By wiring capacitors, which serve as an analogue of a protein, we solder them in a sequence keeping a distance around 1 cm and the long linear array of capacitors is rolled spirally along a cylinder surface keeping a pitch 1.03 cm accurately as shown in Fig. 1a. Thus, we keep pitch-to-diameter ratio as 1.03:1.00, which is abundantly used in the biomaterials as we have seen theoretically from the crystal structure data available for multiple spiral biomaterials. Now, we have reported earlier that microtubule switches its lattice parameters, following which we have replicated two lattice structures in two devices. It is known that a pair of identical coils would make maximum wireless power transfer. In this case, we are not interested in an absolute power transfer, but how exactly power transfer takes places, if at all any. From that context, we need microtubule analogues of different lattices.

There are two unique novelties in our work. First, our device is a junk material as far as electronics is concerned. If we try to pass low-frequency signals or near dc current, it faces an infinite resistance in a capacitor. However, if the frequency increases, the dielectrics switches polarize synchronously with the variation of the applied ac signal passing the wave. Therefore, up to a very high frequency, our device is simply a junk material. Moreover, as we connect a large number of capacitors in series, the lattice network also works as a capacitor and that blocks certain frequency range of ac signals further. Eventually, we end up in creating a system that blocks both ac and dc signals largely. This disadvantage could turn into an advantage. Blocking electrons critically may even help us in generating a field of a new kind. Second, we never use ac or dc signals from highly stable sources, but the noise generated from various noise generators is used for the measurement of signal transmission. Noise has profound effects on the capacitors.

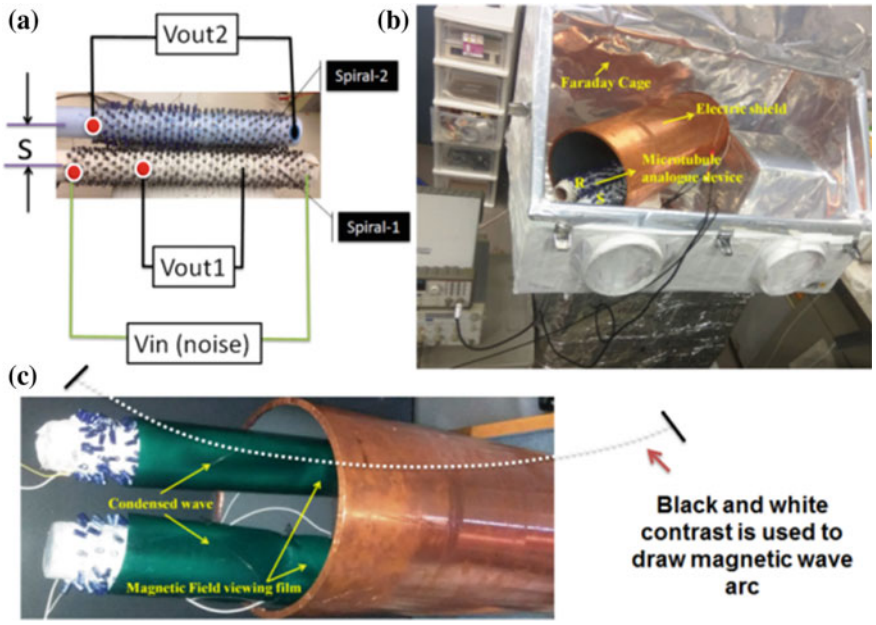

Fig. 1 **a** A pair of microtubule analogue device made of arrayed capacitors with diameter around 5.5 cm and length 30 cm. Vin is the circuit connection through which noise is applied as an input (20–80 mV). Vout is the wiring by which output voltage or signal or charge content measurement is carried out in the device. Another device is kept isolated and Vout is measured as ac signal through function generator, **b** entire device is kept inside a multilayered electromagnetic shielding chamber. Then, for critical measurement to confirm that the truly magnetic condensate is transmitting wirelessly from Spiral 1 to Spiral 2, we used another Cu chamber shown in the panel (**c**). On the green magnetic sensor sheet, if we keep long time, say hours (use new sheet for every experiment, because first experiment is very sensitive, and then there is a permanent hysteresis effect on the sheet), then the magnetic condensate wave is visible. The condensate looks like a waveform as we have shown using a dotted line how the arc looks like, and from the curvature of the condensed waveform we can calculate the wavelength of the condensed wave

2.2 The "Heat Pipe" Effect

Our target is to achieve "heat pipe effect" in the cylindrical surface. In a "heat pipe" effect, [31] a hollow pipe is filled with dielectric, where physical motion of quanta by radiation and transmission is associated with the phase ripples, where no physical objects move. Since the phase part transmits in parallel, the conductivity could reach 100 times that of silver [32]. Capacitors are well studied by exhibiting the heat pipe effect [33]. The phase transition of electrolyte works together to efficiently transfer heat between two neighboring capacitors and in its dielectric between two leads. Water channel increases the conductivity through microtubule by ~10^3 times, the effect of capillary water is significant in heat pipe effect [34]. Phase-assisted heat transfer is wireless and it does not get affected by the path resistance. Additionally,

a spiral path helps in thermal energy storage [35] and [36]. Therefore, we carefully select noise such that it is just sufficient to deplete the capacitors and engage the dielectric in rapid phase transition, so that three events happen. They are: (i) electronic motions are critically arrested, (ii) rapid phase transition increases the phase-assisted heat transfer, and (iii) electrons are critically arrested within the capacitor blocking leakage largely transforming the material from an extreme insulator (10^{12} Ω) to a super nonconductor (10^{15} Ω). The heat pipe effect-based transfer increases inversely with the depletion of electrons. These two fundamentals are background works for the finding presented here.

All along this study, we have been careful to use simple methods so that our striking finding that challenges the very idea of electronics is reproduced by school students everywhere. For that reason, we have bought market available magnetic sensor sheets and wrap up the devices, both the sources, where we apply a noise and the receiver, where we measure a wireless transmission. The magnetic sensor papers accumulate the magnetic moments from the surface of the artificial devices and provide direct evidence that a condensed magnetic wave has been created both in the source and in the destination device. We have used multilayered electromagnetic shields that block major parts of the external signal in a Faraday box. In addition, the study has been looking into the power transfer, estimating the magnetic flux, and finding the relationships between the magnetic condensed waves formed in the source and the destination.

3 Theory of Wireless Transmission

We built a preliminary theory of the phenomenon. Here, we briefly note a few aspects of it. Microtubule undergoes rapid phase changes on its surface. We can consider its surface as a composition of lattices of various lattice parameters and sizes. At a particular resonance frequency, there is an equilibrium, we get $N_r^{equ} = N_0 \exp\left(-\frac{\Delta G_{cluster}(r)}{k_B T}\right)$, this statistically accounts for the composition of lattice symmetries at resonance, where

$$\Delta G_{cluster}(r) = -\Delta G_{lc,v} \cdot \pi r^2 l_{cluster} + \sigma \pi r^2 l_{microtubule}. \tag{1}$$

Here, $\Delta G_{lc,v}$ is due to phase change per unit cluster area on the microtubule surface and σ is the interfacial free energy propagating throughout the microtubule surface due to THz transmissions between tubulin proteins or equivalent capacitors. From Eq. (1), we get $\Delta G_{critical} = \frac{16\pi\sigma^3}{3\Delta G_{lc,v}^2}$, at radius of cluster of a particular lattice configuration would increase ($r > r_c$), i.e., greater than a critical radius, and Eq. (1) predicts a condensation above this limit. Condensation means that a particular lattice starts dominating its surface. The rate of condensation of a typical symmetry in a receiver microtubule's surface is given by

$$G = S_c k N_0 \frac{1}{N_c} \left(\frac{\Delta G_c}{3\pi k_B T} \right)^{1/2} \exp\left(-\frac{\Delta G_c}{k_B T} \right). \tag{2}$$

Here, N_c is the number of lattice points that first synchronizes its phase in the sender with the receiver's magnetic condensed wave's phase. Now, we need to find phase gain rate g_s from the lattice gain rate G. We have explained it in the following.

To understand the wireless communication between the microtubule analogue devices, we have inherently considered the coupled mode theory model of two resonant systems for the analysis. According to this coupled mode theory, these two resonant systems act as a source and receiver as shown in Fig. 1. The source system has a resonant frequency of ω_s. The overall system gain rate is expressed as $G = g_s - \gamma_s$, where g_s is the phase gain rate of the source and γ_s is the intrinsic loss rate of the source. The receiver lattice has a resonant frequency of ω_r. The overall loss rate of the system is expressed as $\gamma = \gamma_r + \gamma_{rl}$, where γ_r is the intrinsic loss rate of the receiver and γ_{rl} is the loss rate at receiver load. Power is transmitted from source to receiver with a transmission coupling coefficient rate α, which is a function of signal amplitude. Transmission coupling coefficient decreases exponentially as the separation distance between source and receiver increases. Here, we have supplied the noise signal to the source. If V_{noise} is the noise signal and V_r is output voltage of receiver, then the rate of change in signals is described by the following equation:

$$\frac{d}{dt} \begin{bmatrix} V_{noise} \\ V_r \end{bmatrix} = \begin{bmatrix} i\omega_s + g_s & -i\alpha \\ -i\alpha & i\omega_r - \gamma \end{bmatrix} \begin{bmatrix} V_{noise} \\ V_r \end{bmatrix}. \tag{3}$$

In Sect. 4, we report all the parameters' results.

4 Avoiding Artifacts

One prime source of artifacts is the environmental noise, as we deal with femto to autto watts. Wireless communications are happening between the source and the destination alone, to prove this, we need to take several precautions, human presence must be avoided, as human body acts as a giant capacitor and movement of a human body transmits power by discharging and charging capacitors. Any laboratory is full of machines, computers to characterization systems, and they radiate huge electromagnetic signals in the entire frequency range. Prior to the experiment, we made an electromagnetic-IR map of the whole room identifying the silent domain and carried out the work.

We used multiple layers of the following seven kinds of materials to create our own ultralow-noise zero Gauss chamber. The chips are kept inside zero Gauss chamber, inside a three-layered Faraday cage. The entire Faraday cage system shown in Fig. 1 is oriented toward the earth's magnetic field. A 2D inductive layer is added on the chamber to trap the ac noise.

(1) MCF7 layer (LF magnetic field, 30 dB (97%)); attenuation HF: 40 dB at 1 GHz, thickness 0.02 mm; permeability: $\mu 4 = 25{,}000$; $\mu max = 100{,}000$; saturation polarization: 0.55 T; and composition: Co69, Fe4, Mo4, Nb1, Si16, and B7. The surface is grounded and it is conducting. (2) Mu layer: Nickel permalloy foil. (3) MCL61 layer: permeability $\mu 2 = 10{,}000$; $\mu 4 = 25{,}000$; $\mu max = 100{,}000$; saturation polarization: 0.55 T; $Hc = 0.5$ A/m; remnant $Br/Bs = 0.7$; and Curie temperature $Tc = 225$ °C. (4) EMF–RF and Ni–Cu ripstop shielding from Faraday defense, which is an electromagnetic shielding. (5) Pure Cu shield from Faraday defense. (6) Brass and aluminum metal sheet was used as core structure of the primary Faraday cage inside which a secondary cage was built. Ar gas 99.99% dry, atmosphere was created between primary and secondary cages. (8) ESD/EMP 7.0MIL material from Faraday defense was custom made at home from DIY kits, using multilayered alternate aluminum and polyester/polyethylene coating as part of primary cage. Two aluminum metal layers in this five-layered bag provide maximum EMP bag protection,—33 lb puncture resistance (FTMS 101-C, 2065.1),—>40 db EMI attenuation (MIL-PFR-81705-REV.D),—surface resistivity (12 Ω/Sq). In (ASTM 1-257),—7 mil thickness (MIL-STD-3010C Method 1003),—moisture barrier (MIL-STD-3010C Method 3030), and heat sealing conditions:—temperature (400 °F, 204 °C),—time (0.6–4.5 s),—pressure (30–70 PSI, 206–482 kPa).

Finally, we studied wireless communication femtowatt (mV, pA) to auttowatt (mV, fA) following various types of measurements and measuring the same event following independent routes. We used amplifiers followed by power meters and sensors, apart from Smith charts of VNA to see if there is a real wireless power transmission. When a large number of capacitors are connected in series, it is expected that no current would flow, and therefore the devices are junk materials. Observation of wireless communication is remarkable and unprecedented.

5 Result and Discussion

Figure 1a shows the experimental setup and two spiral devices are made of 22 μF capacitors. We varied capacitance from 1–100 μF, changed diameters, length, pitch, but for clarity, in this first report, we confine into only one kind of device. One important aspect of this setup is that V_{in} and V_{out} are connected to different instruments (e.g., connect both to an oscilloscope, vector network analyzers, impedance analyzers, spectrum analyzers, etc.) to find the nature of signal produced by noise V_{in} and the transmitted signal. The Cu tube is rotated in Fig. 1b so that the devices kept inside are visible. A pair of analogue microtubule devices kept inside the Cu cylinder is enlarged in Fig. 1c and we can see that both the sender and the receiver devices are wrapped with the magnetic sensor sheet. One peculiarity of this sensor sheet is that it accumulates magnetic flux as the time pass by, it means if the magnetic condensate formed in the device is stable over time, the sheet would integrate and deliver the cumulative response.

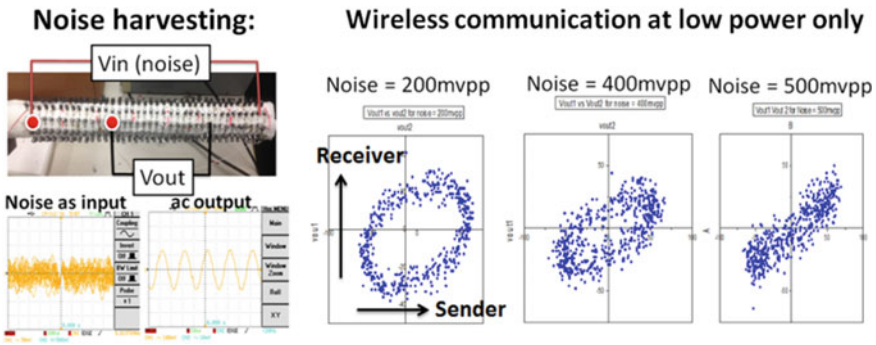

Fig. 2 Two panels are plotted side by side. In the left panel, there are three subpanels, one above shows the measuring circuit and the pair of panels below are the screenshots of the oscilloscope when the system was pumped with random noise (left) as Vin and output are taken as Vout, which is extremely low power (femtowatt) but ordered. This is an evidence that the arrayed capacitors in a lattice form are not a junk device. In the extreme right, three panels are indicating the Lissajous figures created during wireless communication between a pair of microtubule analogue devices. X-axis of an oscilloscope is fed with Vout1 and Y-axis of that oscilloscope is fed with Vout2. Together, they create Lissajous figures. An ellipse in the first panel suggests in phase transfer of wireless signal. Noise is increased 200–500 mV, and the transmitted signal nearly disappears. The unique phenomenon is observed only under noise

Figure 2 shows the noise harvesting basic experiment. Here, noise between 20 and 80 mV is applied in the 1 kHz–50 MHz range (Vin) and then the output is measured (Vout), which is a regularized ordered signal. The electronically junk device that does not have the ability to transmit electron converts noise of a particular type into an ordered signal. This is the most effective form of noise harvesting known to us. Three researchers were not told about the incredible phenomenon and were asked to repeat the experiments, between 2015 and 2017, and the three students reproduced the typical wireless communication parameters in a triple blind experiment. One of the most profound evidence that a unique wireless transmission is taking place in this electronically junk spiral topology is the three right panels of Fig. 2. Here, we have taken output signals from the source and the receiver and feed them in the X and Y axes of the oscilloscope to produce the Lissajous figure with 45° phase difference tells us about the phase locking transport of the ac signal. Now, conventional machines are not equipped with probes to determine the nature of the signal being transported. However, pure magnetic wave is really impossible to find. Only feasible easy to comprehend situation would be, if the magnetic signal is transmitted, which sends information of phase and then the signal rebuilds in the sender. Due to the magnetic nature of signal, phase locking is visible.

To confirm that the transmitted signal is magnetic in nature, we have inserted a pure magnetic metal shield of Ni sheet, and multiple other types of magnetic field absorbers and found that the transmitted signal is affected (Fig. 3a). The separation between the two coils is increased when the signal decreases to a threshold low value, but not zero. Currently, we are investigating distance independent transmission that

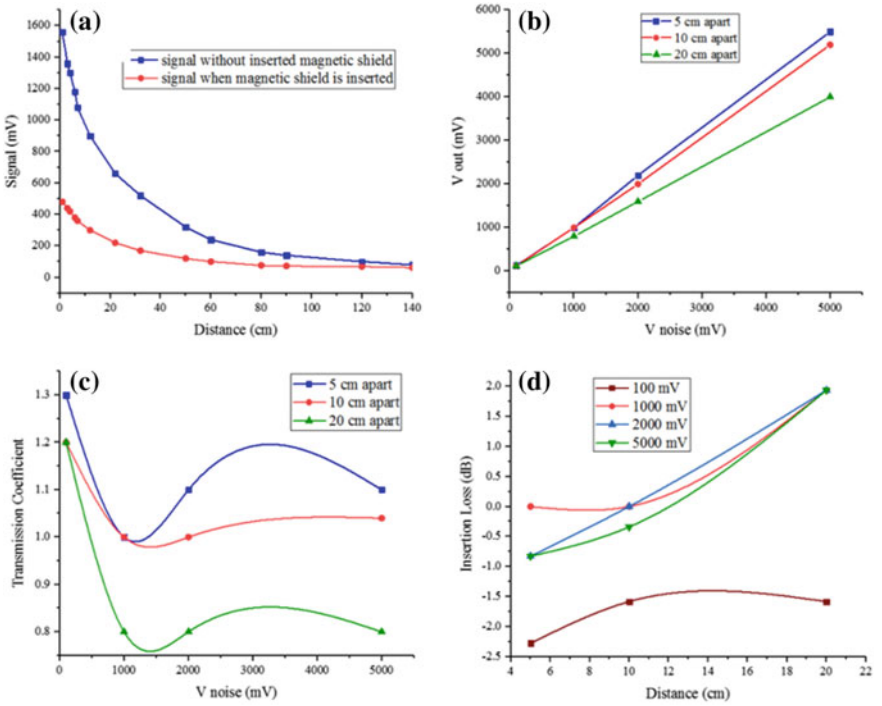

Fig. 3 **a** Two plots (blue, higher signal), when there is no magnetic shielding between the pair of devices that undergo wireless communication tests and when a shield is applied (red, lower signal). **b** Vout or transmitted power variation as a function of input noise for three different separations of sender and receiver coil. The amplitude applied to the device is much higher (around 5 V, because we tested the possibility of wireless communication with high power when device performance degrades due to hysteresis). **c** Transmission coefficient (ratio between output and input) is plotted as a function of noise input for three different separations. **d** Insertion loss (dB) as a function of the separation between the spiral coils for different noise inputs

is a possibility as observed by parity-based wireless communication researchers in other systems, or this is merely an artifact. Nevertheless, we confirm that power does get transmitted magnetically and wirelessly. Figure 3b is an interesting observation, here, a peculiar type of a nearly distance independent feature of wireless transmission is seen at low noise. Readers should note that this particular phenomenon of wireless transfer occurs best at less than 100 mV as shown in Fig. 2, all data in Fig. 3 are taken after tens of hours of continuous monitoring, to get very good image of condensate in our magnetic sensor.

Waiting for several hours provides a very good image of a standing wave of magnetic flux, and one could see transmission between coils even if noise is switched off, which is remarkable. However, the device characterization becomes difficult due to fatigue. Figure 3c is one example of a pair of saturated device undergoing operations for tens of hours. We can see a Gaussian-like response as a function of

Vin or Vnoise, it means even at a very high bias, there is a limiting domain where the phenomenon is observed. But, always, for the best response, a set of fresh devices work on 20–80 mV (shorting does not help in old devices). We have observed similar Gaussian optimization at several domains.

Exponential decay with distance suggests radiative transmission which varies in an inverse square manner with the distance. Figure 3c illustrates the noise voltage versus transmission coefficient graph. The transmission coefficient is the ratio of the transmitted output voltage to the applied noise voltage. Transmission coefficient more than 1 means that after reaching the destination the transmitted power increases. This is another remarkable feature of this new kind of wireless transmission. We activated both the device with noise and then mixed particular ac signal with the noise, even then, the receiver magnifies the signal. It means there is a clear harvesting of noise by the capacitor carpet on the cylindrical surface.

Figure 3d shows a new kind of optimization, which shows a peculiar feature at 100 mV. Here, it is also seen that at 100 mV the transmission coefficient is always greater than 1. Therefore, 100 mV may be considered as an operating voltage of noise, where at a particular separation, there is maximum wireless transmission and there is a domain where increasing the separation increases the transmission. This is possible if phase-assisted transport is happening during wireless transmission, and there is an interference of waves in the post-transmission scenario. One possibility would be phase-assisted transport of THz sensors, and using GaInN diode we have detected the transmission of THz signals across the capacitors. However, real thermal flow is trivial to be regulated in a nonlinear fashion, and the only possibility would be assisting in synchronizing all the capacitors on the cylindrical surface.

We have carried out detailed lattice variation study by changing the capacitor arrangement on the cylindrical surface. Joule heating of a capacitor is maximum during a dc current flow. However, under ripples of an ac signal or noise, a capacitor rapidly heats up and cools down. Rapid heating/cooling leads to a rapid phase transition inside the capacitor, like a heat pipe. Rate of phase transition could modulate conductivity by ~10^3 orders of magnitude [37]. The effects, phase regulation, and automated heat stabilization [38] enable "heat pipe" capacitors as noise harvesting system. In a microtubule, the arrayed proteins are rolled on a water crystal, it enhances the magnetic flux condensation, depicting the phase transfer-based transmission. Microtubule could act as a heat pipe under noise of particular (10–200 MHz; 5–70 GHz) frequency bandwidth, where water crystal activates.

Getting back to Fig. 3d, since it illustrates the distance between microtubule analogue devices versus insertion loss, which tells that how much signal is lost resulting from the insertion of a device, we see a gain instead of loss. Insertion loss of a two-port device can be calculated by the following equation: insertion loss (dB) = −20log|Vout/Vnoise|. It is clear from Fig. 3d that there is a less signal loss at 100 mV input noise voltage. Insertion loss is associated with the deformation of the magnetic wave formed by the condensation of the magnetic wave. Figure 4a illustrates the input noise voltage versus wavelength of condensed wave that we have calculated from the arc, which we measure directly from the helical coil surface. Condensed wave is observed by the magnetic field viewing film, which is placed on

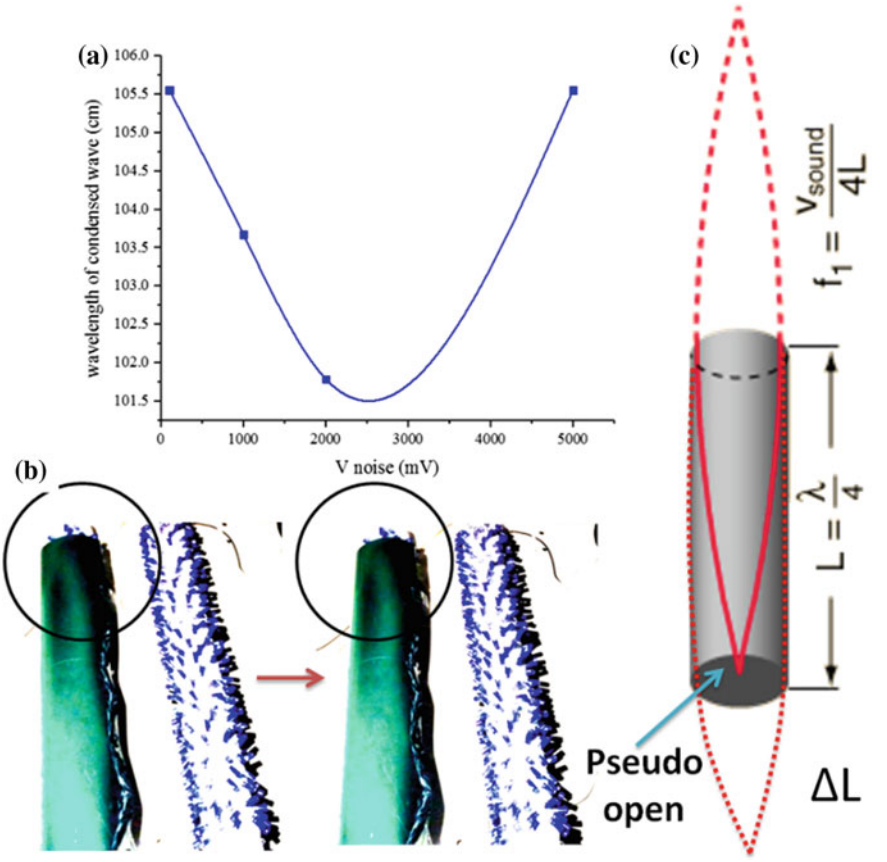

Fig. 4 **a** From the magnetic condensed wave visualized on the magnetic sensor sheet, arc is depicted as shown in the panel Fig. 1c, wavelength is calculated, which could be tuned using a noise amplitude as plotted. **b** Condensate is imaged live for hours, apparently, there is no change, but if there is an animated video, then we can see the change in the waveform shape. **c** Schematic presentation of the condensed wave formed in the microtubule analogue device, we see the condensed wave as if the device is very long (which is not real), and a part of the standing wave is cutoff. We do not know the reason, but it enables the device to generate waves much longer than the device's dimension

the microtubule analogue devices (shown in Fig. 1). More the noise bias is increased, the wavelength decreases and this means that the device squeezes the waveform to accommodate more magnetic energy on the cylindrical surface. This is a clever, intuitive, and a brilliant demonstration of energy management. We plan to explore this particular technology of energy management while developing the commercial version of noise harvesting devices. Topology of the lattices made of capacitors on the cylindrical surface has one unique advantage. There are plenty of different symmetries simultaneously superposed.

We repeat the context of coexistence of multiple symmetries on the cylindrical surface. In the nearest neighborhood scenario, we get one lattice symmetry made by the lattice points or capacitor location. However, there is a cable that is helically passing through noise from the beginning to the end of the array. A dc signal is blocked as soon as the first capacitor is charged, an ac signal would be blocked due to various capacitors formed by the network of wiring throughout the cylindrical surface, but the noise cannot be stopped. Therefore, noise plays a vital role in activating majority of the capacitors rapidly charging and discharging, which is also the foundation of the heat pipe effect. At the same time, noise-induced signals get regularized and several different reflected waves form and flow throughout the cylindrical surface. And we have compiled a random database of such waves only to conclude that the system generates various different waveforms. If we connect both the sender and receiver to the spectrum analyzer and observe 1 kHz–6 GHz simultaneously, we can identify a bunch of peaks not just one. Peaks are around 10–300 MHz. Here, in Fig. 4a when we are presenting the wavelength 100 cm it means we are arguing for around 300 MHz wave.

Another interesting observation that we made was that the magnetic wave that we image does not use the cylindrical surface boundary as a cavity, nor does it use it as a dielectric resonator. Large number of resonance peak and missing part of the waveform pointed out in Fig. 4b and is explained with a simple schematic in Fig. 4c , which suggests that the condensed magnetic wave originates from topology, and a hierarchical integration of phase is not limited to the dimension of the device.

6 Conclusion

We have shown here the magnetic condensate formation and its wireless transfer between a pair of analogue microtubule devices. There would be plenty of applications if a microscale version of this device is made, and one application would be the biomedical engineering and wireless power transfer technology for biomedical implants. In future, we will study modulation of the core of the cylinder with non-magnetic conducting elements mimicking the water crystal located at the core of a microtubular structure. Water has unique dielectric property [39]. We have already demonstrated that without the water channel microtubule loses all its remarkable electronic features [21]. Pentagon rings of water are fundamental to microtubule core, but are fundamental to other proteins too [40]. Water layer around protein molecule is essential and its dielectric property plays a vital role [41]. Protein hydration might have an impact on the wireless transmission and water molecules make an integral part of the molecule [42]. Buried water molecules hold protein's energy landscapes [43].

Acknowledgements We thank Dave Sonntag and Martin Timms for the independent test and verification of our device as part of patent US9019685B2. Authors acknowledge the Asian office of Aerospace R&D (AOARD), a part of United States Air Force (USAF) for the Grant no. FA2386-

16-1-0003 (2016–2019) on the electromagnetic resonance-based communication and intelligence of biomaterials.

References

1. Simic, M., Bil, C., Vojisavljevic,V.: Investigation in wireless power transmission for UAV charging. Proc. Comput. Sci. **60**, 1846–1855 (2015)
2. Jawad, A.M., Nordin, R., Gharghan, S.K., Jawad, H.M., Ismail, M.: Opportunities and challenges for near-field wireless power transfer: a review. Energies **10**(1022), 1–28 (2017)
3. Ho, J.S., Yeh, A.J., Neofytou, E., Kim, S., Tanabe, Y., Patlolla, B., Beygui, R.E., Poon, A.S.Y.: Wireless power transfer to deep-tissue microimplants. PNAS **111**, 7974–7979 (2014)
4. Jiang, H., Zhang, J., Lan, D., Chao, K.K., Liou, S., Shahnasser, H., Fechter, R., Hirose, S., Harrison, M., Roy, S.: A low-frequency versatile wireless power transfer technology for biomedical implants. IEEE Trans. Biomed. Circuits Syst. **7**, 526–535 (2013)
5. Ghosh, S., Chatterjee, S., Roy, A., Ray, K., Swarnakar, S., Fujita, D., Bandyopahyay, A.: Resonant oscillation language of a futuristic nano-machine-module: eliminating cancer cells & Alzheimer Aβ plaques. Curr. Topic. Med. Chem. **15**, 534–541 (2015)
6. Zein, I., Wyman, J.: Studies on the dielectric constant of protein solutions. J. Biol. Chem. **76**, 443–476 (1931)
7. Elliott, M.A., Williams, J.W.: The dielectric behavior of solutions of the protein zein. J. Am. Chem. Soc. **61**, 718–725 (1939)
8. Vollmer, F., Braun, D., Libchaber, A.: Protein detection by optical shift of a resonant microcavity. Appl. Phys. Lett. **80**, 4057–4059 (2002)
9. Schirò, G., Cupane, A., Vitrano, E., Bruni, F.: Dielectric relaxations in confined hydrated myoglobin. J. Phys. Chem. B **113**, 9606–9613 (2009)
10. Kim, Y.-H., Yoon, S-II, Park S., Kim, H-S, Kim, Y-J, Jung, H.-I.: A simple and direct biomolecule detection scheme based on a microwave resonator. Sens. Actuat. B **130**, 823–828 (2008)
11. Lu, Q., Shu, F.-J., Zou, C.-L.: Dielectric Bow-tie nanocavity. Opt. Lett. **38**, 5311–5314 (2013)
12. Verma, R., Daya, K.S.: Rapid detection of pM concentration of insulin, using microwave whispering gallery mode. IEEE Sens. J. **17**, 2758–2765 (2017)
13. Zhai, Z., Kusko, C., Hakim, N., Sridhar, S., Revcolevschi, A., Vietkine, A.: Precision microwave dielectric and magnetic susceptibility measurements of correlated electronic materials using superconducting cavities. Rev. Sci. Instrum. **71**, 3151–3160 (2000)
14. Hanham, S.M., Watts, C., Otter, W.J., Lucyszyn, S., Klein, N.: Dielectric measurements of nanoliter liquids with a photonic crystal resonator at terahertz frequencies. Appl. Phys. Lett. **107**(032903), 1–5 (2015)
15. Burdette, E.C., Cain, F.L., Seals, J.: In vivo probe measurement technique at VHF through microwave frequencies. IEEE Trans. Microw. Theozy Tech. **28**, 414–427 (1980)
16. Ghosh, S., Sahu, S., Agrawal, L., Shiga, T., Bandyopadhyay, A.: Inventing a co-axial atomic resolution patch clamp to study a single resonating protein complex and ultra-low power communication deep inside a living neuron cell of integrative. Neuroscience **15**, 403–433 (2016)
17. Glanz, J.: Force-carrying web pervades living cell. Science **276**, 678–679 (1997)
18. Pokorný, J.: Endogenous electromagnetic forces in living cells: implications for transfer of reaction components. Electro-Magnetobiol. **20**, 59–73 (2001)
19. Pethig, R.: Dielectric and electronic properties of biological materials **139**, p. 376. Wiley, Chichester and New York (1979)
20. Sahu, S., Ghosh, S., Fujita, D., Bandyopadhyay, A.: Live visualizations of single isolated tubulin protein self-assembly via tunneling current: effect of electromagnetic pumping during spontaneous growth of microtubule. Sci. Rep. **4**(7303), 1–9 (2014)

21. Sahu, S., Ghosh, S., Ghosh, B., Aswani, K., Hirata, K., Fujita, D., Bandyopadhyay, A.: Atomic water channel controlling remarkable properties of a single brain microtubule: correlating single protein to its supramolecular assembly. Biosens. Bioelectron. **47**, 141–148 (2013)
22. Ghosh, S., Sahu, S., Fujita, D., Bandyopadhyay, A.: Design and operation of a brain like computer: a new class of frequency-fractal computing using wireless communication in a supramolecular organic, inorganic systems. Information **5**, 28–99 (2014)
23. Tesla, N.: Apparatus for transmitting electrical energy. US patent 1,119,732 (1914)
24. Assawaworrarit, S., Yu, X., Fan, S.: Robust wireless power transfer using a nonlinear parity-time-symmetric circuit. Nature **546**, 387–390 (2017)
25. Kurs, A., Karalis, A., Moffatt, R., Joannopoulos, J.D., Fisher, P., Soljačiic, M.: Wireless power transfer via strongly coupled magnetic resonance. Science **317**, 83–86 (2007)
26. Nair, V.V., Choi, J.R.: An efficiency enhancement technique for a wireless power transmission system based on a multiple coil switching technique. Energies **9**(156), 1–15 (2016)
27. Sample, A.P., Meyer, D.A., Smith, J.R.: Analysis, experimental results, and range adaptation of magnetically coupled resonators for wireless power transfer. IEEE Trans. Industr. Electron. **58**, 544–554 (2011)
28. Hameroff, S.R., Watt, R.C.: Information processing in microtubule. J. Theor. Biol. **98**, 549–561 (1982)
29. Sahu, S., Ghosh, S., Hirata, K., Fujita, D., Bandyopadhyay, A.: Multi-level memory-switching properties of a single brain microtubule. Appl. Phys. Lett. **102**(123701), 1–4 (2013)
30. Sahu, S., Fujita, D., Bandyopadhyay, A.: Inductor made of arrayed capacitors. 2010 Japanese patent has been issued on 20th August 2015 JP-511630 (world patent filed, this is the invention of fourth circuit element), US patent has been issued 9019685B2, 28 April (2015)
31. Heat pipe effect was invented long back by Gaugler, R.S., 1942; further improved by Grover, G., 1963
32. Catalog of Indek Corporation, 1998 holds this particular fact
33. Gasperi, M.L., Gollhardt, N.: Heat transfer model for capacitor banks. In: 33rd Annual Meeting of the IEEE IAS (1998)
34. Wang, Y., Gundevia, M.: Measurement of thermal conductivity and heat pipe effect in hydrophilic and hydrophobic carbon papers. Int. J. Heat Mass Trans. **60**, 134–142 (2013)
35. David, A.: Reay: thermal energy storage: the role of the heat pipe in performance enhancement. Int. J. Low-Carbon Technol. **10**, 99–109 (2015)
36. Zalba, B., Marin, J.M., Cabeza, L.F., Mehling, H.: Review on thermal energy storage with phase change materials, heat transfer analysis and applications. Appl. Therm. Eng. **23**, 251–283 (2003)
37. Udell, K.S.: Heat transfer in porous media considering phase change and capillarity—the heat pipe effect. Int. J. Heat Mass Trans. **28**, 485–495 (1985)
38. Parler, S.G.: Deriving life multipliers for Aluminum electrolytic capacitors. IEEE Power Electron. Soc. Newslett. **16**, 11–12 (2004)
39. Buchner, R., Barthel, J., Stauber, J.: The dielectric relaxation of water between 0 °C and 35 °C. Chem. Phys. Lett. **306**, 57–63 (1999)
40. Teeter, M.M.: Water structure of a hydrophobic protein at atomic resolution: pentagon rings of water molecules in crystals of crambin. Proc. Natl. Acad. Sci. U.S.A. **81**, 6014–6018 (1984)
41. Ebbinghaus, S., Kim, S.J., Heyden, M., Yu, X., Heugen, U., Gruebele, M., Leitner, D.M., Havenith, M.: An extended dynamical hydration shell around proteins. Proc. Natl. Acad. Sci. U.S.A. **104**, 20749–20752 (2007)
42. Otting, G., Liepinsh, E., Wuthrich, K.: Protein hydration in aqueous solution. Science **41**, 974–980 (1991)
43. Denisov, V., Peters, J., Hörlein, H.D., Halle, B.: Using buried water molecules to explore the energy landscape of proteins. Nature. Struct. Biol. **3**, 505–509 (1996)